THE JOURNAL OF PHYSICAL CHEMISTRY Letters

Letter

pubs.acs.org/JPCL

Charge Separation and Recombination at Polymer–Fullerene Heterojunctions: Delocalization and Hybridization Effects

Gabriele D'Avino,[†] Luca Muccioli,[§] Yoann Olivier,[†] and David Beljonne*[,†]

[†]Laboratory for Chemistry of Novel Materials, University of Mons, 7000 Mons, Belgium

[§]Laboratoire de Chimie des Polymères Organiques, UMR 5629, University of Bordeaux, 33607 Pessac, France

Supporting Information

ABSTRACT: We address charge separation and recombination in polymer/fullerene solar cells with a multiscale modeling built from accurate atomistic inputs and accounting for disorder, interface electrostatics and genuine quantum effects on equal footings. Our results show that bound localized charge transfer states at the interface coexist with a large majority of thermally accessible delocalized space-separated states that can be also reached by direct photoexcitation, thanks to their strong hybridization with singlet polymer excitons. These findings reconcile the recent experimental reports of ultrafast exciton separation ("hot" process) with the evidence that high quantum yields do not require excess electronic or vibrational energy ("cold" process), and show that delocalization, by shifting the density of charge transfer states toward larger effective electron–hole radii, may reduce energy losses through charge recombination.

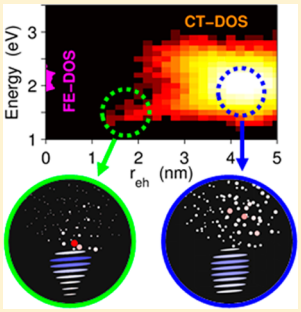

Motivated by the prospects for high-efficiency organic solar cells, there have been considerable efforts to unveil the mechanisms of charge separation at donor/acceptor (D/A) heterojunctions.[1,2] Though this is still a very much debated question, there is growing evidence that, in the best devices, almost quantitative charge photogeneration from relaxed charge-transfer (CT) states occurs without the need for excess electronic or vibrational energy,[3−5] possibly assisted by an entropic gain ensured by the three-dimensional character of the fullerene acceptors.[6,7] This seems to imply that exciton dissociation proceeds through weakly bound CT states, a mechanism supported by microelectrostatic calculations of model interfaces.[8−10] On the other hand, a recent report on charge separation occurring within a 40 fs time window over distances of a few nm in fullerene-based bulk heterojunctions,[11] and other evidence of ultrafast phenomena,[12−14] point instead to the combined role of delocalization effects and vibrationally "hot" states in pulling charges apart.[15−17] Yet, how do we reconcile these two nearly opposite pictures of charge separation? And how do we account in the same framework for the massive recombination of photogenerated charges, which has been identified as the main factor responsible for open-circuit voltage losses[18] and that drastically limits the power conversion efficiency of organic solar cells?

To address these questions, we resort to a full atomistic theoretical description of charge pairs at polymer–fullerene interfaces that accounts on an equal footing for electrostatic, disorder, and delocalization effects. Our modeling reveals the presence of distinct populations of CT states that are involved in the charge separation (CS) and charge recombination (CR) processes. Namely, CS may occur both as a thermally activated process and by direct photoexcitation of space-separated CT states acquiring oscillator strength due to strong mixing with resonant polymer singlet excitons. We further show that CR, which originates from intermolecular couplings among interfacial molecules, should be reduced by charge delocalization that shifts the density of CT states toward larger effective electron–hole (e–h) radii.

The description of the electronic structure at the length scale pertaining to charge separation at organic heterojuctions is a formidable task that we tackle with a multiscale approach grounded on a site-based model Hamiltonian fed with atomistic inputs. Our starting point is the realistic P3HT/PCBM interface in Figure 1a obtained from molecular dynamics simulations,[9] which defines molecular sites and their disordered

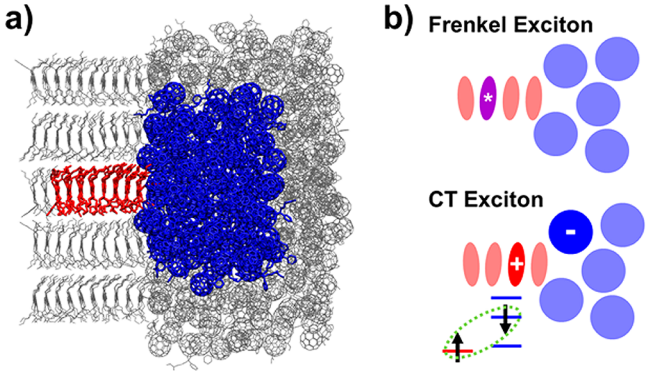

Figure 1. (a) Snapshot of the P3HT/PCBM interface considered in this study; the colored region represents the subsystem described by Hamiltonian (1). (b) Sketch of the molecular Frenkel exciton and singlet-coupled charge transfer states.

Received: December 2, 2015
Accepted: January 18, 2016
Published: January 19, 2016

DOI: 10.1021/acs.jpclett.5b02680
J. Phys. Chem. Lett. 2016, 7, 536−540

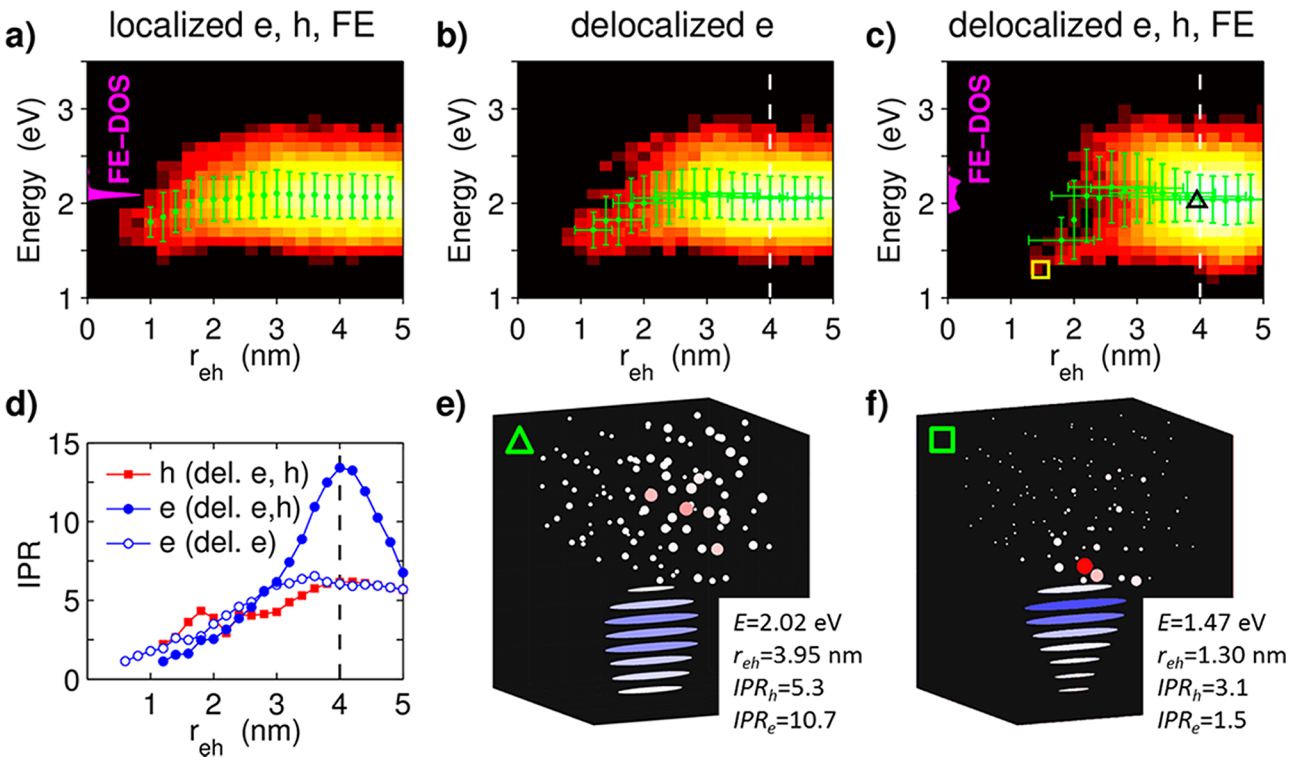

Figure 2. (a–c) Density of pure CT states (heat map, logarithmic color scale) as a function of e–h distance and energy for localized and delocalized carriers. Green dots show the energy profile averaged in intervals of r_{eh}, vertical (horizontal) error bars report the standard deviation of energy (e–h mean spread) within each interval. Magenta areas in panels a and c show the DOS of pure localized and delocalized FEs, respectively. (d) Average inverse participation ratio (IPR) as a function of r_{eh}. (e,f) Rendering of representative CT states, triangle and square recall panel c.

connectivity. The electronic Hamiltonian is represented on a diabatic basis of localized states including the neutral state $|0\rangle$, singlet Frenkel excitons (FE) $|i\rangle$, and singlet-coupled CT states $|i,j\rangle$ with i and j running on D and A sites, respectively. We explicitly consider the three low-lying unoccupied orbitals of fullerene derivatives,[19] so j is actually a composite index labeling A sites and orbitals. On this basis, the Hamiltonian reads

$$H = H_{CT} + H_{FE} + H_{CT-FE} \tag{1}$$

$$H_{CT} = \sum_{i,j} \varepsilon_{ij}^{CT} |i,j\rangle\langle i,j| + \sum_{j} \sum_{\langle i,i'\rangle} J_{ii'}^{h} |i,j\rangle\langle i',j| + \sum_{i} \sum_{\langle j,j'\rangle} J_{jj'}^{e} |i,j\rangle\langle i,j'| + \sum_{i,j} J_{ij}^{g} |0\rangle\langle i,j| \tag{2}$$

$$H_{FE} = \sum_{i} \varepsilon_{i}^{FE} |i\rangle\langle i| + \sum_{\langle i,i'\rangle} J_{ii'}^{x} |i\rangle\langle i'| \tag{3}$$

$$H_{FE-CT} = \sum_{\langle i,j\rangle} J_{ij}^{s} |i\rangle\langle i,j| \tag{4}$$

Where H_{CT} accounts for the energy of electrostatically interacting CT states (diagonal energies ε_{ij}^{CT}), for hole and electron transfer (CT couplings $J_{ii'}^{h}$ and $J_{jj'}^{e}$), and for ground-state charge transfer couplings (J_{ij}^{g}) that are also responsible for CR. H_{FE} is the traditional Frenkel exciton model with site energies ε_{i}^{FE} and energy transfer couplings $J_{ii'}^{x}$, and finally H_{FE-CT} mixes Frenkel and CT excitons via the exciton splitting coupling J_{ij}^{s}.

Although similar models have been recently proposed,[15,20−23] the novelties over previous works are several, the most important being (i) we move away from ideal lattices of reduced dimensionality in favor of the three-dimensional morphology of a realistic P3HT/PCBM interface; (ii) the CT states energies (ε_{ij}^{CT}) include the effect of electrostatic interactions with the polarizable environment as evaluated with classical microelectrostatic calculations;[9,24] (iii) electronic couplings driving charge and energy transfer are computed for molecular pairs extracted from the MD sample and hence explicitly account for structural disorder (see Experimental Section and the Supporting Information (SI)). The proposed theoretical approach, bridging the gap between mesoscale electronic structure models and robust atomistic calculations, represents an important step toward a realistic description of the electronic states and processes at organic D/A interfaces.

We start our discussion from pure CT states, i.e., the eigenstates of H_{CT} in eq 2 that do not present any mixing with FEs. Our calculations confirm a very small CT in the ground state with less than 0.01 electrons of net charge on the D or A subsystem,[21] which corresponds to a negligible vacuum level shift (<5 meV) across the interface. The effect of charge delocalization on the energy landscape of CT states is addressed in Figure 2, where we compare the density of CT states (CT-DOS) computed according to three scenarios: (i) fully localized holes and electrons ($J^{h} = J^{e} = 0$), (ii) delocalized electrons with localized holes ($J^{h} = 0$), and (iii) fully delocalized holes and electrons. The average energy profile in the localized picture (Figure 2a) points to two populations of CT states: a low-energy tail of states with $r_{eh} < 2$ nm that are electrostatically bound by 0.3–0.4 eV, and a dominant fraction of states featuring larger e–h radii and characterized by a rather flat energy profile.[9]

The CT-DOS changes substantially when accounting for delocalization, especially when both electrons and holes can

DOI: 10.1021/acs.jpclett.5b02680
J. Phys. Chem. Lett. 2016, 7, 536−540

spread on multiple molecules. The remarkable difference between the CT-DOS in Figure 2b,c attests to the importance of accounting for the delocalization of both carriers, at least for neat interfaces to large polymer crystallites. However, many polymer/fullerene blends present amorphous polymer domains and phase intermixing, hence we expect the actual scenario to be comprised between the pictures in Figure 2b,c. Delocalization has a favorable effect on charge separation, as it stabilizes less Coulombically bound CT states at large e−h distance and shifts the CT-DOS to larger r_{eh}. Both charge carriers can in fact delocalize toward their respective transporting materials, leading to an increase of the average e−h distance, although many delocalized CT states have tails extending down to the interface. Charge delocalization, quantified by the inverse participation ratio (IPR, see Figure 2d), increases with r_{eh}, leading to CT states whose electronic clouds spread on average over ∼13 fullerenes at $r_{eh} \sim 4$ nm, like the one rendered in Figure 2e. Nevertheless, a small population of more localized and bound CT states at small r_{eh} persists even when both electrons and holes are allowed to delocalize (square in Figure 2c and Figure 2f). This result is consistent with the distance distribution of (relaxed) photogenerated charges obtained by Barker et al.,[25] from the analysis of low-temperature recombination dynamics.

With a realistic description of the CT-DOS at hand, we can now turn our attention to FEs. Because of the strong energy transfer couplings between P3HT decamers ($J^x \approx 80$ meV), pure FEs (eigenstates of H_{FE}, eq 3) spread over the polymer stack leading to very different FE-DOS in the localized ($J^x = 0$ in eq 3, magenta area in Figure 2a) and delocalized picture (Figure 2c). The nature of the electronic excitations radically changes upon switching on the coupling with CT states (H_{FE-CT}), which leads to strong FE-CT *hybridization* as measured by their fractional FE (CT) character ν_{FE} (ν_{CT}). We quantify the number of excited states of nearly pure FE character ($\nu_{FE} > 0.9$) to be only the 32% of that of (pure and localized) basis FEs. While these numbers are specific to our model interface and system-size dependent, we point out that the disappearance of pure FE in the close proximity of an interface is instead a general result, as also suggested by many-body Bethe−Salpeter calculations on bimolecular complexes.[26] The weight of FEs of interfacial polymer chains is therefore dispersed in the manifold of CT states, which, due to their much larger number, maintain mostly $\nu_{CT} \sim 1$.

Strongly hybridized excitations should efficiently mediate the ultrafast conversion of pure FE generated in the polymer bulk in high-energy CT states,[27] but also strongly affect the optical properties of the D/A interface. Figure 3a shows the absorption cross section calculated for our P3HT/PCBM interface, which resembles the P3HT H-aggregate absorption associated with FEs, plus a weak low-energy tail due to the intrinsic CT absorption. The intense polymer absorption is polarized along the backbone axis, while CT features also have an out-of-plane component. Even though this is fully consistent with optical measurements,[3] our modeling further reveals that much of the absorption intensity comes from states with a large CT character borrowing their intensity from bright FEs: for our P3HT/PCBM interface the 62% of the integrated cross-section is provided by states with $\nu_{CT} > 0.5$. Moreover, most of this absorption corresponds to CT states with an effective e−h distance larger than 3 nm and that are resonant with FE. This is better shown by the r_{eh}-resolved absorption spectrum of hybrid CT states in Figure 3b, which reveals the correlation between

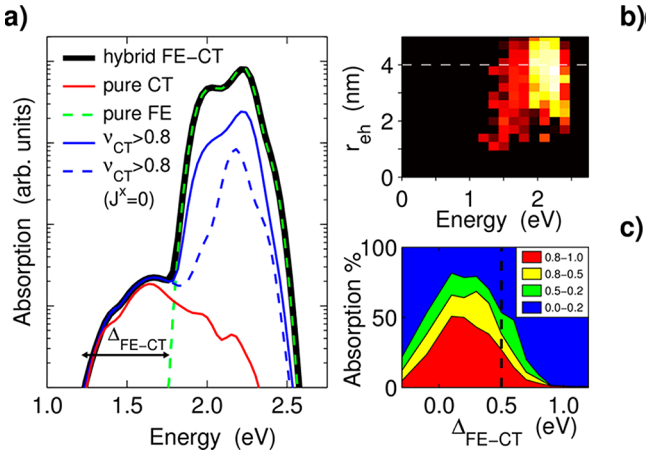

Figure 3. (a) Absorption spectrum of the P3HT/PCBM interface computed with different models (see text). (b) Absorption spectrum of hybrid CTEs resolved in energy and e−h distance, showing that most of CT transitions mainly yields space separated charges. (c) Participation of states of different CT character (ν_{CT} in the caption) to the total absorption cross-section as a function of Δ_{FE-CT}. The vertical line at $\Delta_{FE-CT} = 0.5$ corresponds to P3HT/PCBM. For $\Delta_{FE-CT} \sim 0.2$ half of the total absorption corresponds to states with $\nu_{CT} > 80\%$.

absorption frequency and the effective distance between the photogenerated e−h pair.

This result confirms the possibility that primary photoexcitations in organic heterojunctions consist in space-separated CT states as suggested by Ma and Troisi for a model two-dimensional D/A interface.[20] The efficient optical generation of space-separated carriers requires delocalized CT states extending down to the interface where these can mix with the FEs,[20] but also other material parameters play a key role. The offset between CT and FE absorptions, which can vary much in polymer/fullerene heterojunctions, is in fact also crucial for achieving large FE-CT mixing. Its effect is addressed in Figure 3c, where we show that the amount of absorption intensity transferred to CT states is maximized for an optimal overlap between CT and FE DOSs. The delocalization of FEs is also very important, as it mediates the coupling between CT states and FEs of the inner polymer chains. Consequently, the absorption intensity of CT states is expected to drop in systems featuring localized excitations, as illustrated in Figure 3a where we compare the cross section of the excited states of prevailing CT character ($\nu_{CT} > 0.8$) in the case of delocalized (full blue line) and localized FEs ($J^x = 0$, blue dashed line).

We next address the critical aspect of charge recombination (CR), which is responsible for voltage losses up to 0.7 eV in organic solar cells.[18] Despite several theoretical attempts to compute CR rates,[28−32] the role of delocalization has been overlooked so far. Here, radiative and nonradiative CR rates from all the excited states have been calculated in both cases of localized and delocalized carriers. In the localized picture, nonzero CR rates are found only for the few CT states corresponding to D/A pairs in close contact at the interface, while sizable rates are found also for delocalized states with $r_{eh} \geq 3$ nm. Following Burke et al.,[18] we assume thermal equilibrium between Coulombically bound CT states and space-separated delocalized charges, both described within our model, and compute Boltzmann averaged (non)radiative rates ($\bar{k}_{NR}$) $\bar{k}_{RAD}$ that are given in Table 1. Our results are in overall accordance with experimental values[18,25] and confirm that the

DOI: 10.1021/acs.jpclett.5b02680
J. Phys. Chem. Lett. 2016, 7, 536−540

Table 1. Thermally Averaged Radiative and Nonradiative CR Rates in s^{-1} Computed for the P3HT/PCBM Interface for Localized and Delocalized Carriers

	localized e and h	delocalized e	delocalized e and h
$\bar{k}_{RAD}$	1.1×10^{6}	5.9×10^{5}	2.3×10^{5}
$\bar{k}_{NR}$	3.0×10^{10}	2.2×10^{10}	4.8×10^{7}

nonradiative pathway is the dominant one. Delocalization is found to reduce $\bar{k}_{NR}$ by 3 orders of magnitude due to the dilution of interfacial localized CT states into the dense manifold of low-energy space separated charges.

Before concluding, we discuss to what extent our results for a specific and ideal P3HT/PCBM heterojunction can be generalized to polymer/fullerene solar cells, starting from the interface morphology. Fullerene typically forms disordered 3D clusters, while soluble π-conjugated polymers aggregate in ordered lamellae or form amorphous and possibly intermixed regions characterized by loose electronic connectivity among polymer segments. Our model calculations, including the intermediate case of electron-only delocalization, capture these essential and general features of polymer−fullerene blends. Other general characteristics are the disordered intermolecular packing, and the reduction of the e−h separation energy barrier provided by the polarization of the microscopic environment, which are both missing in standard lattice models.

Two key quantities that may be strongly system-dependent are the relative energies and couplings of FE and CT absorption features, which we vary in a broad range, and the electrostatic potential probed by charge carriers at the interface.

For our rather neat P3HT/PCBM interface, the electrostatic potential is energetically favorable to e−h separation, substantially reducing the corresponding energy barrier by about 0.4 eV. This result depends, however, on several factors (i.e., materials chemical structure, interface morphology, and macroscopic shape) and variations of similar magnitude, either favoring or disfavoring e−h separation energy-wise, have been computed[32,33] or measured[34,35] for other systems. Although the energy and distance distribution of CT states (and hence CR rates) depends on the details of the electrostatic landscape, the coexistence of bound localized CT states and delocalized space-separated charges are general features we found also for the ideal case of a uniform interfacial electrostatic landscape (see SI).

In summary, our modeling reveals the presence of states of different nature at organic D/A heterojunctions, namely, bound localized CT states at the interface and a large majority of delocalized space-separated states; pure molecular FEs barely exist in the close proximity of the interface and their absorption intensity is largely transferred to resonant CT states. This provides a key for interpreting the early branching in the fate of photogenerated CT states observed for several polymer/fullerene blends[12,25] and reconciles the observations of charge separation in the ultrafast and thermally activated regime, while showing that charge delocalization may slow down charge recombination. The emerging picture confirms the crucial role of CT states and their energetics that is largely governed by electrostatic interactions and morphology. High-energy CT states, mostly superimposed to the polymer absorption, are pivotal for achieving high charge yields, minimizing at the same time voltage losses.

EXPERIMENTAL SECTION

Parameters in eqs 1−3 were obtained from calculations performed on the structures of the MD-simulated P3HT/PCBM interface in ref 9. FE energies and charge and energy transfer couplings were evaluated at the semiempirical INDO/S level. $\bar{k}_{NR}$ was computed with a Marcus−Levich−Jortner formula suitably modified to account for delocalization,[36] $\bar{k}_{RAD}$ was computed assuming spontaneous emission. Results were obtained for 10 supramolecular clusters similar to that in Figure 1a, sampling the whole interface of ref 9.

ASSOCIATED CONTENT

Supporting Information

The Supporting Information is available free of charge on the ACS Publications website at DOI: 10.1021/acs.jpclett.5b02680.

Comprehensive computational details, distribution of charge and energy transfer couplings, energetics of localized CT states, system size effects, and additional results (PDF)

AUTHOR INFORMATION

Corresponding Author

*E-mail: David.Beljonne@umons.ac.be.

Notes

The authors declare no competing financial interest.

ACKNOWLEDGMENTS

The work in Mons was supported by the Programme d'Excellence de la Reǵion Wallonne (OPTI2MAT Project) and FNRS-FRFC. G.D. acknowledges support from EU through the FP7-PEOPLE-2013-IEF program (GA 2013-625198). D.B. is research director of FNRS. The work in Bordeaux has been funded by French National Grant ANR-10-LABX-0042-AMADEus managed by the National Research Agency under the initiative of excellence IdEx Bordeaux programme (Reference ANR-10-IDEX-0003-02).

REFERENCES

(1) Brédas, J.-L.; Norton, J. E.; Cornil, J.; Coropceanu, V. Molecular Understanding of Organic Solar Cells: The Challenges. *Acc. Chem. Res.* **2009**, *42*, 1691−1699.

(2) Clarke, T. M.; Durrant, J. R. Charge Photogeneration in Organic Solar Cells. *Chem. Rev.* **2010**, *110*, 6736−6767.

(3) Lee, J.; Vandewal, K.; Yost, S. R.; Bahlke, M. E.; Goris, L.; Baldo, M. A.; Manca, J. V.; Voorhis, T. Van. Charge Transfer State versus Hot Exciton Dissociation in Polymer-Fullerene Blended Solar Cells. *J. Am. Chem. Soc.* **2010**, *132*, 11878−11880.

(4) Van Der Hofstad, T. G. J.; Di Nuzzo, D.; van den Berg, M.; Janssen, R. A. J.; Meskers, S. C. J. Infl Uence of Photon Excess Energy on Charge Carrier Dynamics in a Polymer-Fullerene Solar Cell. *Adv. Energy Mater.* **2012**, *2*, 1095−1099.

(5) Vandewal, K.; Albrecht, S.; Hoke, E. T.; Graham, K. R.; Widmer, J.; Douglas, J. D.; Schubert, M.; Mateker, W. R.; Bloking, J. T.; Burkhard, G. F.; et al. Efficient Charge Generation by Relaxed Charge-Transfer States at Organic Interfaces. *Nat. Mater.* **2014**, *13*, 63−68.

(6) Gregg, B. A. Entropy of Charge Separation in Organic Photovoltaic Cells: The Benefit of Higher Dimensionality. *J. Phys. Chem. Lett.* **2011**, *2*, 3013−3015.

(7) Monahan, N. R.; Williams, K. W.; Kumar, B.; Nuckolls, C.; Zhu, X.-Y. Direct Observation of Entropy-Driven Electron-Hole Pair Separation at an Organic Semiconductor Interface. *Phys. Rev. Lett.* **2015**, *114*, 247003.

(8) Verlaak, S.; Beljonne, D.; Cheyns, D.; Rolin, C.; Linares, M.; Castet, F.; Cornil, J.; Heremans, P. Electronic Structure and Geminate

DOI: 10.1021/acs.jpclett.5b02680
J. Phys. Chem. Lett. 2016, 7, 536−540

Pair Energetics at Organic−Organic Interfaces: The Case of Pentacene/C60 Heterojunctions. *Adv. Funct. Mater.* **2009**, *19*, 3809−3814.
(9) D'Avino, G.; Mothy, S.; Muccioli, L.; Zannoni, C.; Wang, L.; Cornil, J.; Beljonne, D.; Castet, F. Energetics of Electron−Hole Separation at P3HT/PCBM Heterojunctions. *J. Phys. Chem. C* **2013**, *117*, 12981−12990.
(10) Castet, F.; D'Avino, G.; Muccioli, L.; Cornil, J.; Beljonne, D. Charge Separation Energetics at Organic Heterojunctions: On the Role of Structural and Electrostatic Disorder. *Phys. Chem. Chem. Phys.* **2014**, *16*, 20279−20290.
(11) Gelinas, S.; Rao, A.; Kumar, A.; Smith, S. L.; Chin, A. W.; Clark, J.; van der Poll, T. S.; Bazan, G. C.; Friend, R. H. Ultrafast Long-Range Charge Separation in Organic Semiconductor Photovoltaic Diodes. *Science* **2014**, *343*, 512−516.
(12) Bakulin, a. a.; Rao, a.; Pavelyev, V. G.; van Loosdrecht, P. H. M.; Pshenichnikov, M. S.; Niedzialek, D.; Cornil, J.; Beljonne, D.; Friend, R. H. The Role of Driving Energy and Delocalized States for Charge Separation in Organic Semiconductors. *Science* **2012**, *335*, 1340−1344.
(13) Jailaubekov, A. E.; Willard, A. P.; Tritsch, J. R.; Chan, W.-L.; Sai, N.; Gearba, R.; Kaake, L. G.; Williams, K. J.; Leung, K.; Rossky, P. J.; et al. Hot Charge-Transfer Excitons Set the Time Limit for Charge Separation at Donor/acceptor Interfaces in Organic Photovoltaics. *Nat. Mater.* **2013**, *12*, 66−73.
(14) Grancini, G.; Maiuri, M.; Fazzi, D.; Petrozza, A.; Egelhaaf, H.-J.; Brida, D.; Cerullo, G.; Lanzani, G. Hot Exciton Dissociation in Polymer Solar Cells. *Nat. Mater.* **2013**, *12*, 29−33.
(15) Tamura, H.; Burghardt, I. Ultrafast Charge Separation in Organic Photovoltaics Enhanced by Charge Delocalization and Vibronically Hot Exciton Dissociation. *J. Am. Chem. Soc.* **2013**, *135*, 16364−16367.
(16) Huix-Rotllant, M.; Tamura, H.; Burghardt, I. Concurrent Effects of Delocalization and Internal Conversion Tune Charge Separation at Regioregular Polythiophene−Fullerene Heterojunctions. *J. Phys. Chem. Lett.* **2015**, *6*, 1702−1708.
(17) Falke, S. M.; Rozzi, C. A.; Brida, D.; Maiuri, M.; Amato, M.; Sommer, E.; De Sio, A.; Rubio, A.; Cerullo, G.; Molinari, E.; et al. Coherent Ultrafast Charge Transfer in an Organic Photovoltaic Blend. *Science* **2014**, *344*, 1001−1005.
(18) Burke, T. M.; Sweetnam, S.; Vandewal, K.; McGehee, M. D. Beyond Langevin Recombination: How Equilibrium Between Free Carriers and Charge Transfer States Determines the Open-Circuit Voltage of Organic Solar Cells. *Adv. Energy Mater.* **2015**, *5*, 201500123.
(19) D'Avino, G.; Olivier, Y.; Muccioli, L.; Beljonne, D. Do Charges Delocalize over Multiple Molecules in Fullerene Derivatives? *J. Mater. Chem. C* **2016**, DOI: 10.1039/C5TC03283K.
(20) Ma, H.; Troisi, A. Direct Optical Generation of Long-Range Charge-Transfer States in Organic Photovoltaics. *Adv. Mater.* **2014**, *26*, 6163−6167.
(21) Raos, G.; Casalegno, M.; Idé, J. An Effective Two-Orbital Quantum Chemical Model for Organic Photovoltaic Materials. *J. Chem. Theory Comput.* **2014**, *10*, 364−372.
(22) Savoie, B. M.; Rao, A.; Bakulin, A. a.; Gelinas, S.; Movaghar, B.; Friend, R. H.; Marks, T. J.; Ratner, M. a. Unequal Partnership: Asymmetric Roles of Polymeric Donor and Fullerene Acceptor in Generating Free Charge. *J. Am. Chem. Soc.* **2014**, *136*, 2876−2884.
(23) Bittner, E. R.; Silva, C. Noise-Induced Quantum Coherence Drives Photo-Carrier Generation Dynamics at Polymeric Semiconductor Heterojunctions. *Nat. Commun.* **2014**, *5*, 3119.
(24) D'Avino, G.; Muccioli, L.; Zannoni, C.; Beljonne, D.; Soos, Z. G. Electronic Polarization in Organic Crystals: A Comparative Study of Induced Dipoles and Intramolecular Charge Redistribution Schemes. *J. Chem. Theory Comput.* **2014**, *10*, 4959−4971.
(25) Barker, A. J.; Chen, K.; Hodgkiss, J. M. Distance Distributions of Photogenerated Charge Pairs in Organic Photovoltaic Cells. *J. Am. Chem. Soc.* **2014**, *136*, 12018−12026.
(26) Duchemin, I.; Blase, X. Resonant Hot Charge-Transfer Excitations in Fullerene-Porphyrin Complexes: Many-Body Bethe-Salpeter Study. *Phys. Rev. B: Condens. Matter Mater. Phys.* **2013**, *87*, 245412.
(27) Chen, K.; Barker, A. J.; Reish, M. E.; Gordon, K. C.; Hodgkiss, J. M. Broadband Ultrafast Photoluminescence Spectroscopy Resolves Charge Photogeneration via Delocalized Hot Excitons in Polymer:-fullerene Photovoltaic Blends. *J. Am. Chem. Soc.* **2013**, *135*, 18502−18512.
(28) Lemaur, V.; Steel, M.; Beljonne, D.; Brédas, J. L.; Cornil, J. Photoinduced Charge Generation and Recombination Dynamics in Model Donor/acceptor Pairs for Organic Solar Cell Applications: A Full Quantum-Chemical Treatment. *J. Am. Chem. Soc.* **2005**, *127*, 6077−6086.
(29) Yi, Y.; Coropceanu, V.; Brédas, J.-L. Exciton-Dissociation and Charge-Recombination Processes in pentacene/C60 Solar Cells: Theoretical Insight into the Impact of Interface Geometry. *J. Am. Chem. Soc.* **2009**, *131*, 15777−15783.
(30) Liu, T.; Troisi, A. Absolute Rate of Charge Separation and Recombination in a Molecular Model of the P3HT/PCBM Interface. *J. Phys. Chem. C* **2011**, *115*, 2406−2415.
(31) Liu, T.; Cheung, D. L.; Troisi, A. Structural Variability and Dynamics of the P3HT/PCBM Interface and Its Effects on the Electronic Structure and the Charge-Transfer Rates in Solar Cells. *Phys. Chem. Chem. Phys.* **2011**, *13*, 21461−21470.
(32) Idé, J.; Méreau, R.; Ducasse, L.; Castet, F.; Bock, H.; Olivier, Y.; Cornil, J.; Beljonne, D.; D'Avino, G.; Roscioni, O. M.; et al. Charge Dissociation at Interfaces between Discotic Liquid Crystals: The Surprising Role of Column Mismatch. *J. Am. Chem. Soc.* **2014**, *136*, 2911−2920.
(33) Poelking, C.; Andrienko, D. Design Rules for Organic Donor-Acceptor Heterojunctions: Pathway for Charge Splitting and Detrapping. *J. Am. Chem. Soc.* **2015**, *137*, 6320−6326.
(34) Burke, T. M.; McGehee, M. D. How High Local Charge Carrier Mobility and an Energy Cascade in a Three-Phase Bulk Heterojunction Enable 90% Quantum Efficiency. *Adv. Mater.* **2014**, *26*, 1923−1928.
(35) Sweetnam, S.; Graham, K. R.; Ngongang Ndjawa, G. O.; Heumuller, T.; Bartelt, J. A.; Burke, T. M.; Li, W.; You, W.; Amassian, A.; Mcgehee, M. D. *J. Am. Chem. Soc.* **2014**, *136*, 14078−14088.
(36) Caruso, D.; Troisi, A. Long-Range Exciton Dissociation in Organic Solar Cells. *Proc. Natl. Acad. Sci. U. S. A.* **2012**, *109*, 13498−13502.

DOI: 10.1021/acs.jpclett.5b02680
J. Phys. Chem. Lett. 2016, 7, 536−540